Organic & Biomolecular Chemistry

PAPER

View Article Online
View Journal | View Issue

Cite this: *Org. Biomol. Chem.*, 2018, **16**, 2470

(Super)gelators derived from push–pull chromophores: synthesis, gelling properties and second harmonic generation†

A. Belén Marco,[a] Denis Gindre,[b] Konstantinos Iliopoulos,[b] Santiago Franco,[a] Raquel Andreu,*[a] David Canevet*[b] and Marc Sallé*[b]

Received 30th January 2018,
Accepted 12th March 2018

DOI: 10.1039/c8ob00251g

rsc.li/obc

The present work takes advantage of the self-assembly process occurring along organogelation, to organize Second Harmonic Generation (SHG) active chromophores. To do so, three push–pull chromophores endowed with a dodecyl urea chain were synthesized and characterized. Their organogelating properties were studied in a wide range of solvents. Despite similar architectures, these derivatives exhibit very different gelling properties, from supergelation to the absence of gelling ability. The utilization of the Hansen solubility parameters allows for observing clear relationships between the gelled solvents and critical gelation concentrations. By evaporating the solvents from the organogels, xerogel materials were prepared and systematically studied by means of optical and electron microscopy as well as SHG microscopy. These studies demonstrate the critical role of the solvent over material structuring and allow generalizing the approach exploiting organogelation as a structuring tool to spontaneously organize push–pull chromophores into SHG-active materials.

Introduction

Low molecular weight organogelators (LMWGs) have increasingly gained attention over the last two decades due to their specific and appealing features.[1–5] They notably show interest in drug delivery,[6] crystallization engineering,[7] pollutant removal,[8] self-healing materials,[9,10] tissue regeneration,[11] or organic electronics[12] and photonics.[13] In the latter fields, their strong potential mainly lies on their ability to form supramolecular polymers during the gelation process.[14] Once the solvent evaporates, the as-prepared organic material, *i.e.* a xerogel, basically consisting of intertwined nano- and microfibers, displays a well-defined organization at the supramolecular scale. Therefore, the preparation of an organogelator endowed with a given functional unit constitutes a method to organize these molecular fragments in an anisotropic manner and reach a desired arrangement. This singular aspect allowed for major breakthroughs in organic electronics with a whole generation of semiconducting and metallic nano- and microwires,[12] which find application in the fields of photovoltaics[15] or sensors[16] for example.

As far as organizing π-functional units into unidimensional structures is concerned, organogelators are also associated with exciting results in the context of organic photonics. For instance, various photostimulable organogels proved to show gel–sol transitions upon irradiation.[17] The gel state also allowed the preparation of materials with increased quantum yields of emission through aggregation-induced emission,[13] improved efficiencies in upconversion processes,[18] or endowed with wave guiding properties.[19] Still in the context of photonics, we recently described gel-based materials derived from **A**, **B** and **C** (Scheme 1), which display a Second Harmonic Generation (SHG) response.[20,21] To generate a second harmonic with such chromophores, it is generally necessary to process the materials with sophisticated techniques to reach a non-centrosymmetric state, which is requisite to observe the phenomenon.[22] In previous studies based on Disperse Red 1 (DR1) derivatives, we demonstrated that such heavy processes can be avoided by designing suitable organogelators, which were able to spontaneously self-assemble into SHG-active xerogels after a simple drop-casting and evaporation sequence. Compound **A**, which includes a push–pull azobenzene chromophore derived from DR1 and a urea-dodecyl gelling fragment, allowed us to deliver a proof of principle.[20] This strategy was subsequently extended to DR1 derivatives **B** and **C**, which include other

[a]*Departamento de Química Orgánica, ICMA, Universidad de Zaragoza-CSIC, 50009 Zaragoza, Spain. E-mail: randreu@unizar.es*
[b]*MOLTECH-Anjou Laboratory, UMR CNRS 6200, University of Angers, 2 bd Lavoisier, 49045 Angers Cedex, France. E-mail: david.canevet@univ-angers.fr, marc.salle@univ-angers.fr*

†Electronic supplementary information (ESI) available: Hansen solubility parameters, additional optical and scanning electron micrographs. See DOI: 10.1039/c8ob00251g

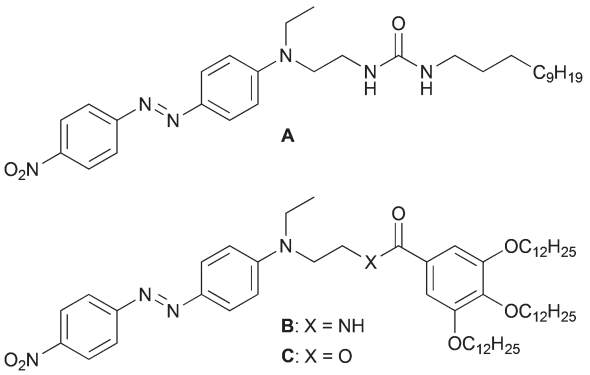

Scheme 1 Chemical structures of previously reported gelators **A–C**.[20,21]

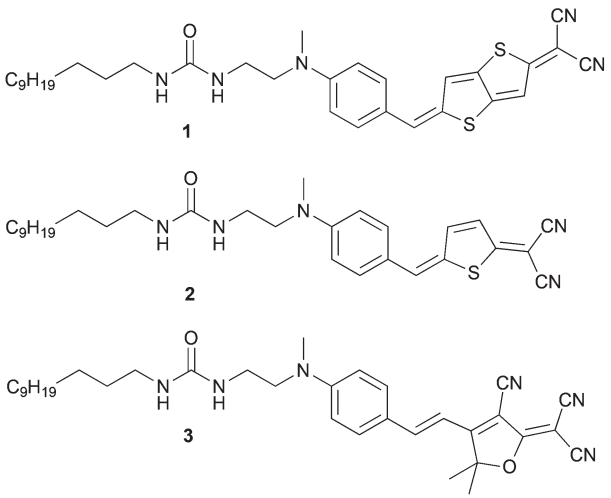

Scheme 2 Chemical structures of targeted compounds **1–3**.

gelling moieties.[21] The results presented herein show that the scope of our approach can be extended to other push–pull systems displaying a non-linear optical activity (Scheme 2).[23,24] Chromophores featuring a quinoidal character (**1** and **2**) appeared as a particularly relevant choice since previous studies showed that quinoid spacers promote efficient intramolecular charge transfers, bathochromically shifted absorption in the UV-visible region and higher nonlinear optical responses.[23,25]

Results and discussion

Synthesis

By analogy with the synthesis of compounds **A–C**, the first considered retrosynthesis to prepare urea-based derivatives **1–3** relied on a final addition reaction involving dodecyl isocyanate and the corresponding amines. This strategy was tested to prepare **1** according to Scheme 3. The initial step consisted of a condensation reaction between azide **4**[26] and dicyanomethylthienothiophene **5**[27] in acetic anhydride, affording **6** with a moderate yield (24%). The reduction of the azide function was subsequently tried through the Staudinger reaction to obtain the corresponding amine. The complete insolubility of the isolated solid prevented any characterization. Therefore, attempts were performed to synthesize **1** by the addition of dodecyl isocyanate in dry dichloromethane over this solid, but this approach proved to be unsuccessful. To circumvent this issue and be able to characterize different intermediates, an alternative retrosynthesis, which is based on the formation of the push–pull system in the last step (Scheme 4), was considered with a main advantage: aldehyde **7** constitutes a common key intermediate to prepare all target derivatives **1–3** in a single step. The aldehyde function of **4** was first protected in the presence of glycol and *p*-toluene sulfonic acid (PTSA) monohydrate in a Dean–Stark apparatus (**8**, 88%) (Scheme 5). The subsequent reduction of **8** under the standard conditions allowed the isolation of amine **9** with 78% yield. Then, the urea moiety was generated through nucleophilic addition over dodecyl isocyanate in dry dichloromethane, to afford **10** with a good yield (76%).[28] Its aldehyde function was subsequently deprotected to yield key intermediate **7** (30%).[29] The latter was successfully reacted with 2-dicyanomethylthiophene **11**[27] in absolute ethanol (63%) and acceptor **12**[30] was condensed in the same solvent in the presence of acetic acid and pyridine (77%). As for chromophore **1**, we were not able to detect its formation

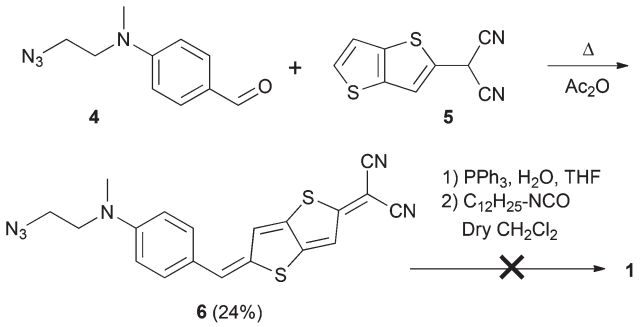

Scheme 3 First strategy followed to prepare chromophore **1**.

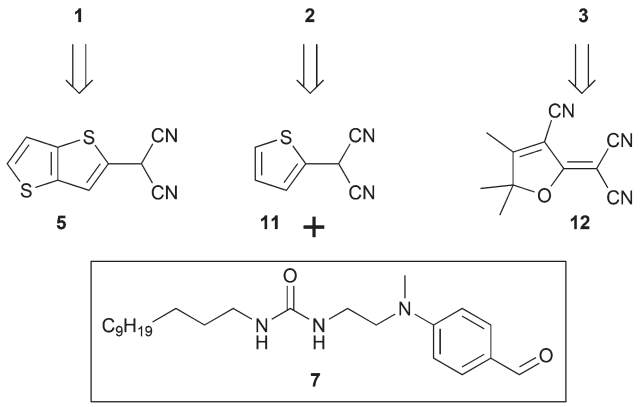

Scheme 4 Alternative retrosynthesis involving intermediate **7**.

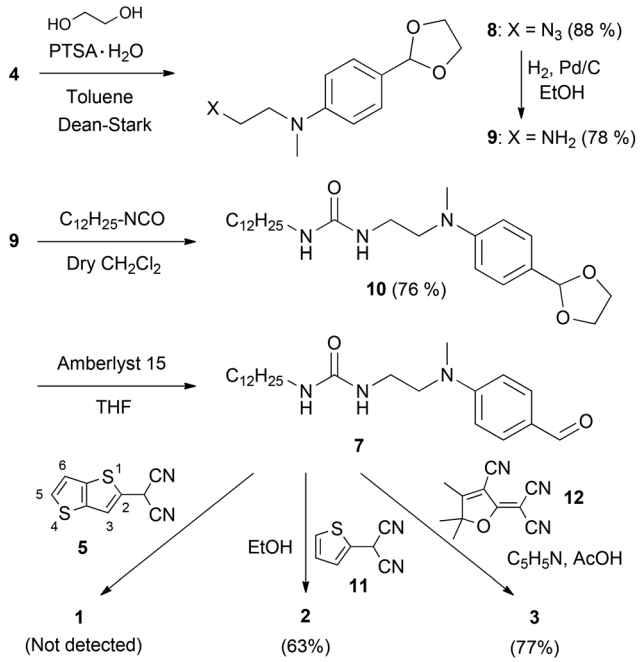

Scheme 5 Synthetic scheme followed to prepare **1–3**.

despite several attempts summed up in Table S1.† One will note that the conditions reported to synthesize an analogous chromophore devoid of an urea-dodecyl moiety[23] did not allow obtaining target compound **1**. Moreover, under the mildest conditions, *i.e.* in absolute ethanol at room temperature, or in chloroform in the presence of silica under microwave heating, a regioisomer of compound **1** (see Scheme S1†) was detected by ^{1}H NMR spectroscopy. To prevent the formation of this isomer and favour grafting at the desired position, thienothiophene-based reagent **15**, endowed with methyl blocking groups on the 3- and 6-positions, was synthesized according to Scheme 6. In an autoclave, 2,5-dimethylhex-3-yn-2,5-diol was heated in the presence of elemental sulfur and benzene at 200 °C to yield 3,6-dimethylthieno[3,2-*b*]thiophene **13** (13%).[31] Following a procedure reported by Seed and coworkers with analogous derivatives,[32] the action of *N*-iodosuccinimide (NIS) over **13** in a mixture of chloroform and acetic acid allowed the isolation of **14** with 75% yield. The dicyanomethyl moiety was subsequently introduced in the presence of sodium hydride, malononitrile and bis(triphenylphosphine)palladium(II) chloride (17%).[27] The last step consisted of performing the condensation reaction of **15** on aldehyde **7** under conditions that had allowed for detecting the regioisomer of target compound **1** (Table S1†). This strategy proved to be valuable since mixing both reagents in refluxing absolute ethanol allowed for isolating target compound **1′** (51%). The chemical structures of intermediates and target derivatives were confirmed through standard analytical techniques (see the Experimental section).

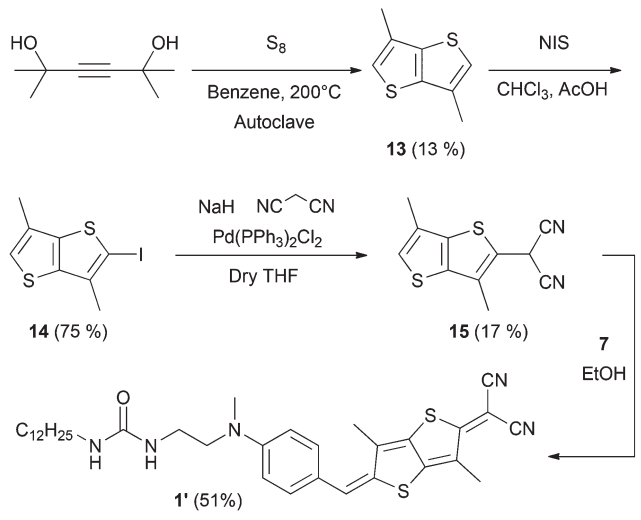

Scheme 6 Synthetic scheme followed to prepare chromophore **1′**.

Phase behaviour in solvents

Both the chemical structures and the methods used to process the corresponding materials must be tuned to reach specific properties.[33] On this basis, we explored the phase behaviours of compounds **1′**, **2** and **3** in a wide variety of solvents. When gelation was observed, the corresponding critical gelation concentration was systematically determined through the inverted vial method (Table 1). At first glance, it appears that derivative **3** does not form any gel, despite the fact that concentrations as high as 80 mg mL^{-1} (chloroform or dioxane), or 100 mg mL^{-1} (tetrahydrofuran or carbon tetrachloride) were tested. A main structural difference exists between **1′**, **2** and **3** since push–pull systems in gelators **1′** and **2** display a quinoidal structure and are planar. Regarding the latter, such a planarity is likely to favour intermolecular interactions through π–π stacking while two methyl groups can impede such contacts in the case of

Table 1 Phase behaviour of compounds **1′–3**. NS indicates that the powder did not dissolve at high temperatures. G stands for gel (the critical gelation concentrations (CGCs) are given between brackets in g L^{-1}), P for precipitate and S for soluble (no gelation was observed up to 50 mg mL^{-1})

Solvents	**1′**	**2**	**3**
Hexane	NS	NS	NS
Cyclohexane	NS	NS	NS
Toluene	G (3.3)	P	P
p-Xylene	P	P	P
Chlorobenzene	G (1.1)	P	S
o-Dichlorobenzene	G (0.6)	G (10.6)	P
1,2,4-Trichlorobenzene	G (0.9)	G (17.7)	P
Chloroform	G (5.8)	P	S
Carbon tetrachloride	G (1.3)	P	S
1,1,2,2-Tetrachloroethane	P	P	S
Acetonitrile	P	G (6.8)	P
Acetone	P	G (13.3)	P
Ethyl acetate	P	P	P
1,4-Dioxane	P	P	S
Tetrahydrofuran	G (8.0)	S	S
Methanol	P	G (13.0)	S
Ethanol	P	P	S
Propan-2-ol	P	P	P
Octan-1-ol	P	P	P

3.[34,35] In any case, the absence of quinoidal character does not explain the absence of gelling properties on its own since the non-quinoidal push–pull system **A** did form gels.

Organogelators **1′** and **2** proved to be soluble at high temperatures in all solvents but alkanes, and displayed very different gelling properties. Gelator **1′** had a clear tendency to gel chlorinated solvents, while **2** afforded gels in miscellaneous solvents, without obvious correlation. Over the last few years, Bouteiller and coworkers have extended the use of Hansen solubility parameters to understand the gelling properties of LMWGs.[36,37] Therefore, we tried to rationalize our observations in light of this theory by plotting the solubility data in the Hansen space (Table S2 and Fig. S1†). To do so, we plotted the tested solvents in a three-dimensional graph, where the coordinates are δ_H, δ_p and δ_d, *i.e.* Hansen solubility parameters. The latter respectively translate the ability of a given solvent to interact through hydrogen bonding, polar interactions and dispersion forces. For both organogelators, some tendencies were observable since, in each case, all gelled solvents belong to the same region of the Hansen space. Gelator **1′** tended to gel solvents displaying a low ability to interact through hydrogen bonds, with maximum δ_H values of 8.0155 and 5.7195 $MPa^{1/2}$ for tetrahydrofuran and chloroform, *i.e.* the solvents that showed the largest critical gelation concentrations (8 and 5.8 mg mL^{-1}, respectively). Conversely, when considering the δ_d and δ_p solubility parameters for gelled solvents, one will observe that they are relatively high in comparison with non-gelled solvents. Altogether, these observations underline the need for both an efficient solvation of the gelling molecule and the preservation of the hydrogen bonding ability of **1′**. Organogelator **2** exhibited an unexpected behaviour since it gels solvents that do not belong to the same sphere in the Hansen space. Interestingly, plotting a projection of the same graph according to the δ_d axis (Fig. S2†) suggests that a frontier exists between the gelled solvents and the others and hence, that a correlation between the solvent properties and gelling ability exists.

To quantitatively assess the respective gelling abilities of **1′** and **2** in different solvents, the required weight percentages of gelators and their gelation numbers (GN)[38] were calculated (Table 2). Exceptional gelating properties are found for **1′**. In particular, the latter is able to gel several solvents with a weight percentage below 0.1%[39] (carbon tetrachloride, 1,2,4-trichlorobenzene (TCB) and 1,2-dichlorobenzene (*o*-DCB)), therefore classifying this compound in the supergelator family. One will also note that the gelation number for compound **2** increases with the Hansen solubility parameter δ_p, which illustrates the solvent ability to interact with a solute through dipolar forces.

Table 2 Weight percentages required to gel solvents with derivatives **1′** and **2** and the corresponding gelation numbers[a]

1′			**2**			
Solvent	%w	GN[a]	Solvent	%w	GN[a]	δ_p ($MPa^{1/2}$)
THF	0.89	931	TCB	1.61	235	6
$CHCl_3$	0.39	1291	*o*-DCB	0.81	434	6.31
Toluene	0.38	1721	Acetone	1.66	531	10.4
CCl_4	0.08	4802	MeOH	1.61	988	12.32
TCB	0.06	5362	CH_3CN	0.86	1463	18.04
CB[b]	0.1	5413				
o-DCB	0.05	8900				

[a] The gelation number corresponds to the number of solvent molecules gelled by a single gelator molecule. [b] CB stands for chlorobenzene.

Xerogels and their microscopic characterization

As mentioned before, the solvent may have a dramatic impact on the obtained xerogel structures.[40] To evaluate the influence of this parameter, optical microscopy constitutes a first valuable tool (Fig. 1, S3 and S4†). To perform these measurements, samples were systematically prepared by drop-casting a warm solution of the gelator (C = critical gel concentration) over a glass slide. The first assessment lies on the radically different microstructures obtained depending on the quite different solvent/gelator since clear monodimensional structures that are locally collinear one to each other could be observed. The birefringence of these structures demonstrates their anisotropy couple under consideration (Fig. S3 and S4†). In chlorobenzene and toluene, organogelator **1′** was prone to form films, which did not display any defined structure under non-polarized light (Fig. 1a and b). Under polarized light (Fig. 1c and d), their organized character was observed. In *o*-dichlorobenzene, chloroform and carbon tetrachloride, heterogeneous films were obtained. While fibrillary structures were clearly observed in the case of carbon tetrachloride, the structures obtained from *o*-dichlorobenzene and chloroform did not seem fibril-

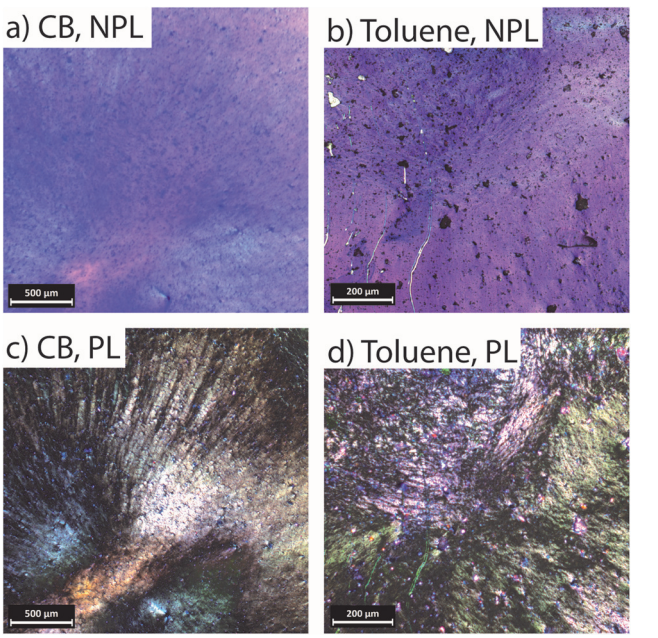

Fig. 1 Optical micrographs of **1′**-based xerogels prepared from chlorobenzene (CB) and toluene under non-polarized (NPL) and polarized (PL) light.

lary structures at first glance. In this regard, scanning electron microscopy (SEM) (Fig. S5†) proved to be valuable since it allowed the imaging of the thin films that could not be observed by optical microscopy and which are located between larger objects. As for the microstructures prepared from 1,2,4-trichlorobenzene and tetrahydrofuran, these appeared spread and well dispersed over the glass slide, weaving a dense network of fibres. In the former case, the material was composed of two types of structures, *i.e.* small particles displaying a diameter of about 10 μm and microwires between the particles (length ≈ 20 μm; diameter ≈ 2 μm) (Fig. S6†). Both types proved to be visible through polarized light optical microscopy, confirming their short scale ordering (Fig. S6†).

Regarding compound **2**, the solvent also strongly affected the material structuring (Fig. S4†). For instance, in *o*-dichlorobenzene and acetone, fibrillary structures were easily observed by optical microscopy (for SEM micrographs, see Fig. 2), while hardly observable with other solvents. The evaporation of 1,2,4-trichlorobenzene and acetonitrile from the gels afforded structures which were hardly imaged by optical microscopy given their thicknesses. However, thin purple fibres could be observed at the periphery of larger objects in the former solvent, and monodimensional structures could be distinguished in the case of acetonitrile when studying these samples under polarized light (Fig. S7†). To confirm this last assertion, SEM micrographs were recorded and did demonstrate the occurrence of a dense network of micro and nanofibers in acetonitrile (Fig. 2). Eventually, the sample prepared with methanol turned out to be a particular case. Indeed, a very smooth film was obtained when drop-casting a warm solution of gelator **2** in this solvent. The specific interaction between the latter and glass provoked a fast spread of the solution over the substrate in comparison with other solvents. This could explain why such a thin and smooth material was produced. Consequently, optical microscopy could not help in imaging the fibres that are responsible for gelation and motivated us to record the corresponding SEM micrograph (Fig. 2b), which also shows a fibrillary microstructure.

Second harmonic generation (SHG) properties

The previously described experimental setup[20] was modified as specified in the Experimental part (see also Fig. S8†) to record the SHG micrographs of the different xerogels. A major difference with our previous SHG studies lies on the fact that the second harmonic generation response is no longer recorded in a transmission mode. Studying the SHG activity of thick materials, which may absorb or scatter the second harmonic, was consequently facilitated. The xerogels were studied through this technique and the corresponding optical and SHG micrographs are presented in Fig. 3 and Tables S3 and 4.† Despite the casting of a warm solution of the gelator and the subsequent evaporation of the solvent, a SHG response could be observed with all xerogels (Fig. 3). Given that non-centrosymmetry constitutes a *sine qua non* condition to detect a SHG response, the interactions driving the supramolecular polymerization and the gelation phenomenon definitely led to a non-centrosymmetric character and hence, SHG-active materials. Such a feature, already observed with bis(diarylamine)-based chromophores[41] or Disperse Red-based xerogels,[20,21] demonstrates that our approach, which consists of grafting a gelling fragment to SHG active chromophores, con-

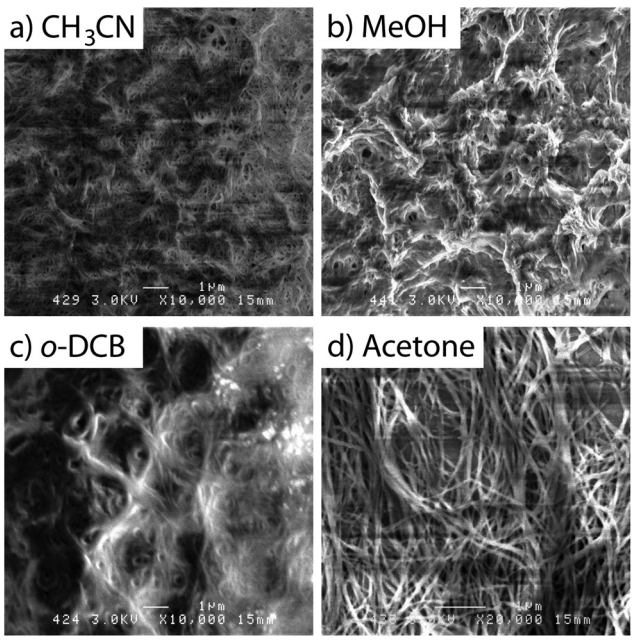

Fig. 2 SEM micrographs of **2**-based xerogels obtained from acetonitrile (a), methanol (b), *o*-dichlorobenzene (c) and acetone (d).

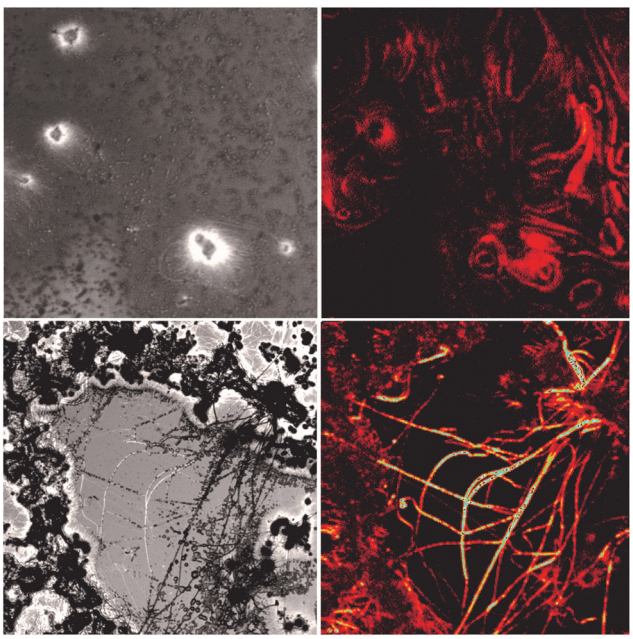

Fig. 3 Optical (left) and SHG (right) micrographs of xerogels prepared from **1′** (top) and **2** (bottom) (same zone) after the evaporation of *o*-dichlorobenzene. These images have the same scale and are 360 μm wide.

stitutes a relevant strategy for promoting spontaneous SHG through organogelation. Moreover, these results show that such a concept can be extended to various classes of chromophores. Finally, it has to be noted that though certain microstructures could not be observed by SHG microscopy, optical and SHG micrographs match irrespective of the solvent under consideration. This results from the fact that second harmonic generation is a polarization dependent phenomenon. Hence, it was possible to tune the SHG response of a given microstructure by simply rotating the polarization of the incident laser (Fig. S9†).

Conclusions

We successfully synthesized and characterized three new push–pull chromophores endowed with urea-dodecyl moieties **1′**, **2** and **3**. The difficulties encountered to prepare thienothiophene-based gelator **1** were circumvented by blocking the 3- and 6-positions of the thienothiophene unit. In this manner, we were able to orient its reactivity and obtain the desired regioisomer **1′**. Targets **1′** and **2** proved to gel a wide range of solvents, with a peculiar emphasis on **1′**, which constitutes a supergelator. By comparing their gelling abilities and plotting the solvents under consideration in the Hansen space, we could establish relevant relationships to rationalize the gelling properties and tendencies regarding the critical gelation concentrations. The critical role of the solvent regarding material processing and structuring could be evidenced. Eventually, nonlinear optical properties could be shown from the corresponding materials through SHG microscopy, demonstrating that the design of appropriate SHG active organogelators constitutes an efficient strategy to afford materials that can spontaneously generate a second harmonic, without the need for sophisticated techniques.

Experimental

Materials and methods

Starting materials were purchased and used without further purification. Thin-layer chromatography (TLC) was performed on aluminium plates coated with Merck Silica gel 60 F254. When necessary, silica gel 60 (35–70 mesh, SDS) was used to isolate the desired derivatives. ^{1}H and ^{13}C NMR spectra were recorded using deuterated solvents as internal references on a BRUKER Advance DRX 300 or a BRUKER AV400 spectrometer. Multiplicities are denoted as follows: s = singlet, d = doublet, t = triplet, m = multiplet, br = broad. The mass spectra were recorded on a Q-ToF spectrometer (accurate mass measurements were achieved using sodium formate as the internal reference), a Jeol JMS 700 (high-resolution mass spectra (HRMS)) or a Bruker Biflex III spectrometer (MALDI-TOF). The infrared absorption spectra were recorded on an FTIR BRUKER VERTEX 70. Optical microscopy was performed by using a Leica DM 2500P microscope. SEM micrographs were recorded by scanning electron microscopy (SEM) with a JEOL JSM 6301F operating at a tension of 3 kV.

Second harmonic generation (SHG) microscopy

The microscope used to record SHG micrographs corresponds to a previously reported setup,[20] which was modified.

Given the thickness and opaque character of certain samples, the setup was modified in order to allow the detection of the reflected SHG signal. To do so, a removable dichroic mirror was implanted on a commercial microscope (IX 71, Olympus) using specific parts 3D printed (Fig. S8†). A 3D-printed optical block was also inserted between the microscope and the photomultiplier (Fig. S8†). It supports a low pass filter (FESH0450, Thorlabs), a 400 nm bandpass filter (FB400-40, Thorlabs) and a lens that focuses the beam on the cathode photomultiplier. Aiming at constructing multi-pass images through the pixel-by-pixel addition of each scan, the acquisition program was modified. It should be noted that an image obtained from only one scan does not display a sufficient contrast. In contrast, performing multi-pass imaging, one can obtain very well contrasted micrographs. This technique permits one to obtain SHG images under specific conditions: in the presence of very low excitation intensities, with materials displaying weak nonlinear responses, or with unstable materials. The images presented in this study were built from 100 successive scans of the area of interest.

Synthetic procedures

Organogelator 1′. Absolute ethanol (3 mL) was added at room temperature under an argon atmosphere to a mixture of aldehyde **7** (85 mg, 0.22 mmol) and **15** (51 mg, 0.22 mmol). The solution was refluxed for 19 hours and concentrated *in vacuo*. Target compound **1′** was isolated by silica gel chromatography (eluent: $CHCl_3$/MeOH 99/1) as a green solid displaying a metallic sheen with 51% yield (67 mg).

M.p. 198–200 °C. IR (ATR) cm^{-1}: 2194 (C≡N). ^{1}H-NMR (300 MHz, $CDCl_3$, 343 K) δ (ppm): 7.53 (d, J = 8.9 Hz, 2H), 7.03 (s, 1H), 6.83 (d, J = 8.9 Hz, 2H), 4.58–4.49 (m, 1H), 4.32–4.23 (m, 1H), 3.62 (t, J = 5.7 Hz, 2H), 3.50–3.40 (m, 2H), 3.18–3.06 (m, 5H), 2.37 (s, 3H), 2.32 (s, 3H), 1.36–1.21 (m, 20H), 0.94–0.83 (m, 3H). ^{13}C-NMR (75 MHz, DMSO-d_6) δ (ppm): 158.0, 151.5, 142.8, 132.9, 131.5, 121.3, 112.3, 83.1, 59.4, 54.8, 38.0, 31.3, 31.2, 29.9, 29.1, 29.0, 28.9, 28.7, 28.6, 26.4, 26.1, 22.0, 21.9, 13.9, 13.5. HRMS (ESI$^+$) m/z: calc. for $C_{34}H_{46}N_5OS_2$ $[M + H]^+$: 604.3144, found: 604.3131.

Organogelator 2. Aldehyde **7** (90 mg, 0.23 mmol) was added to a solution of compound **11** (38 mg, 0.25 mmol) in absolute ethanol (20 mL) under an argon atmosphere. The medium was maintained at room temperature for 18 hours and concentrated *in vacuo*. Silica gel chromatography (eluent: chloroform/methanol 99/1) was used to isolate organogelator **2** as a purple solid (70 mg, 63%).

M.p. 164–166 °C. IR (ATR) cm^{-1}: 2201 (C≡N), 1686 (C=O). ^{1}H-NMR (300 MHz, $CDCl_3$) δ (ppm): 7.50 (d, J = 9.1 Hz, 2H), 7.33 (d, J = 5.4 Hz, 1H), 7.22 (s, 1H), 7.01 (d, J = 5.4 Hz, 1H),

6.82 (d, J = 9.1 Hz, 2H), 4.39–4.29 (m, 1H), 4.24–4.14 (m, 1H), 3.66–3.59 (m, 2H), 3.46–3.38 (m, 2H), 3.13–3.07 (m, 5H), 1.49–1.38 (m, 2H), 3.31–3.20 (m, 18H), 0.88 (t, J = 6.8 Hz, 3H). ^{13}C-NMR (75 MHz, $CDCl_3$) δ (ppm): 147.8, 136.6, 133.3, 129.7, 125.6, 112.5, 52.2, 45.0, 40.8, 38.8, 38.0, 37.9, 31.9, 30.1, 29.7, 29.6, 29.6, 29.5, 29.5, 29.4, 29.3, 29.2, 26.9, 22.7, 14.1. HRMS (ESI^+) m/z: calc. for $C_{30}H_{41}N_5OS$ [$M^{+\bullet}$]: 519.3032, found: 519.3042.

Compound 3. Pyridine (560 μL, 7 mmol) and acetic acid (280 μL, 4.9 mmol) were added to a solution of aldehyde **7** (200 mg, 0.5 mmol) and acceptor **2** (120 mg, 0.6 mmol) in absolute ethanol (25 mL). The medium was heated to reflux under an argon atmosphere for 18 hours. The solvent was evaporated under reduced pressure and the residue was dissolved in a minimum of dichloromethane. Hexane was added to provoke precipitation and the suspension was filtered. The solid was rinsed with hexane to obtain pure **3** as a purple solid (225 mg, 77%).

M.p. 128–130 °C. IR (ATR) cm^{-1}: 2224 (C≡N). ^{1}H-NMR (300 MHz, $CDCl_3$) δ (ppm): 7.60 (d, J = 15.1 Hz, 1H), 7.53 (d, J = 9.0 Hz, 2H), 6.81 (d, J = 9.0 Hz, 2H), 6.72 (d, J = 15.1 Hz, 1H), 4.47–4.39 (m, 1H), 4.27–4.19 (m, 1H), 3.69–3.58 (m, 2H), 3.48–3.36 (m, 2H), 3.14 (s, 3H), 3.12–3.05 (m, 2H), 1.75 (s, 6H), 1.34–1.17 (m, 20H), 0.88 (t, J = 6.8 Hz, 3H). ^{13}C-NMR (75 MHz, $CDCl_3$) δ (ppm): 176.3, 174.2, 158.1, 153.4, 148.4, 132.4, 124.9, 122.0, 112.4, 112.0, 111.5, 108.6, 96.9, 93.9, 52.3, 40.7, 38.9, 37.9, 36.5, 31.9, 30.9, 30.2, 29.7, 29.6, 29.5, 29.3, 26.9, 26.7, 22.7, 14.1. HRMS (ESI^+) m/z: calc. for $C_{34}H_{47}N_6O_2$ [M + H]$^+$: 571.3760, found: 571.3754; calc. for $C_{34}H_{46}N_6NaO_2$ [M + Na]$^+$: 593.3580, found: 593.3770.

Azide 6. To a mixture of aldehyde **4** (50 mg, 0.25 mmol) and 2-dicyanomethylthieno[3,2-*b*]thiophene **5** (50 mg, 0.248 mmol) under an argon atmosphere, acetic anhydride (1.5 mL) was added. The mixture was heated to reflux and stirred for 1 hour and then slowly cooled to room temperature. Hexane was added and the resulting solid was filtered off and washed with hexane. The crude product was purified by flash column chromatography (silica gel) using hexane/CH_2Cl_2 2 : 8 as the eluent to afford azide **6** (23 mg, 24%) as a blue solid. ^{1}H NMR (300 MHz, $CDCl_3$): 8.34 (s, 1H), 7.74–7.71 (m, 2H), 7.20 (s, 1H), 7.00 (s, 1H), 6.81–6.78 (m, 2H), 3.68 (t, J = 5.9 Hz, 2H), 3.56 (t, J = 5.9 Hz, 2H), 3.18 (s, 3H).

Aldehyde 7. Compound **10** (794 mg, 1.8 mmol) was dissolved in tetrahydrofuran (10 mL) and anhydrous Amberlyst 15 was added at room temperature. The mixture was stirred for 15 minutes before filtration. The resin was rinsed with dichloromethane (50 mL) and the filtrate was concentrated *in vacuo*. Aldehyde **7** was isolated by silica gel chromatography (eluent: first, $CHCl_3$, then, $CHCl_3$/MeOH 99/1) as a white powder with 30% yield (211 mg).

M.p. 72–74 °C. IR (KBr) cm^{-1}: 3334 (–NH), 1678, 1661 (C═O). ^{1}H-NMR (400 MHz, $CDCl_3$) δ (ppm): 9.70 (s, 1H), 7.69 (d, J = 9.0 Hz, 2H), 6.75 (d, J = 9.0 Hz, 2H), 4.59 (t, J = 5.9 Hz, 1H), 4.38 (t, J = 5.5 Hz, 1H), 3.59 (t, J = 6.4 Hz, 2H), 3.44–3.37 (m, 2H), 3.14–3.08 (m, 2H), 3.07 (s, 3H), 1.48–1.39 (m, 2H), 1.29–1.22 (m, 18H), 0.87 (t, J = 6.9 Hz, 3H). ^{13}C-NMR (100 MHz, $CDCl_3$) δ (ppm): 190.3, 158.1, 153.8, 132.2, 125.3, 111.0, 52.1, 40.7, 38.7, 38.0, 31.9, 30.2, 29.7, 29.6, 29.4, 26.9, 22.7, 14.2. HRMS (ESI^+) m/z: calc. for $C_{23}H_{40}N_3O_2$ [M + H]$^+$: 390.3115, found: 390.3096; calc. for $C_{23}H_{39}NaN_3O_2$ [M + Na]$^+$: 412.2934, found: 412.2916.

Compound 8. A solution of aldehyde **4** (0.97 g, 4.75 mmol), ethylene glycol (0.73 g, 11.85 mmol) and *p*-toluene sulfonic acid monohydrate (0.154 g, 0.81 mmol) in toluene (35 mL) was refluxed under an inert atmosphere for 17 hours. After cooling down to room temperature, a saturated solution of sodium hydrogenocarbonate (60 mL) was added. The aqueous phase was extracted three times with ethyl acetate (50 mL). The combined organic layers were washed with water (3 × 50 mL), dried over magnesium sulfate and concentrated *in vacuo*. In this manner, the relatively unstable compound **8** was obtained with 88% yield (1.03 g).

IR cm^{-1}: 2097 (–N_3), 1616 (C═C, Ar), 1520 (C═C, Ar), 1178 (C–O). ^{1}H-NMR (400 MHz, $CDCl_3$) δ (ppm): 7.35 (d, J = 8.7 Hz, 2H), 6.71 (d, J = 8.7 Hz, 2H), 5.73 (s, 1H), 4.16–4.10 (m, 2H), 4.04–3.98 (m, 2H), 3.55 (t, J = 6.0 Hz, 2H), 3.44 (t, J = 6.0 Hz, 2H), 3.02 (s, 3H). ^{13}C-NMR (100 MHz, $CDCl_3$) δ (ppm): 149.2, 127.7, 125.8, 111.8, 104.1, 65.2, 51.9, 48.7, 38.9. HRMS (ESI^+) m/z: calculated for $C_{12}H_{17}N_4O_2$ [M + H]$^+$: 249.1346, found: 249.1354.

Compound 9. To a solution of azide **8** (1.033 g, 4.2 mmol) in absolute ethanol, palladium over 10% charcoal was added (1.04 g) at room temperature under a hydrogen atmosphere. The mixture was stirred for 10 hours and filtered through Celite and concentrated *in vacuo*. The desired compound (722 mg, 78%) was used in the next step without further purification as a light brown oil.

IR cm^{-1}: 3361 (–NH), 3299 (–NH), 1614 (C═C Ar), 1178 (C═O). ^{1}H-NMR (400 MHz, $CDCl_3$) δ (ppm): 7.32 (d, J = 8.8 Hz, 2H), 6.71 (d, J = 8.8 Hz, 2H), 5.72 (s, 1H), 4.15–4.09 (m, 2H), 4.03–3.96 (m, 2H), 3.81–3.63 (m, 2H), 3.43 (t, J = 6.5 Hz, 2H), 2.91 (s, 3H), 2.83 (t, J = 6.5 Hz, 2H). ^{13}C-NMR (100 MHz, $CDCl_3$) δ (ppm): 150.3, 127.6, 125.2, 111.9, 104.2, 65.1, 52.9, 47.2, 38.7. MS (ESI^+) m/z: 223.0 [M + H]$^+$.

Compound 10. Compound **9** (722 mg, 3.25 mmol) was dissolved in dry dichloromethane (15 mL) and dodecyl isocyanate (0.9 mL, 3.6 mmol) was added at room temperature under an inert atmosphere. The mixture was stirred for 14 hours and concentrated *in vacuo*. The residue was dispersed in pentane and isolated by filtration as a white solid (1.072 g, 76%).

^{1}H-NMR (400 MHz, $CDCl_3$) δ (ppm): 7.34 (d, J = 8.8 Hz, 2H), 6.68 (d, J = 8.8 Hz, 2H), 5.72 (s, 1H), 4.16–4.10 (m, 2H), 4.04–3.97 (m, 2H), 3.53–3.44 (m, 2H), 3.43–3.32 (m, 2H), 3.08–2.98 (m, 2H), 2.93 (s, 3H), 1.34–1.11 (m, 20H), 0.88 (t, J = 6.8 Hz, 3H). MS (ESI^+) m/z: 434.2 [M + H]$^+$.

Compound 13. In an autoclave, 2,5-dimethylhex-3-yn-2,5-diol (4.26 g, 30 mmol) and sulfur (2.38 g, 74 mmol) were dispersed in benzene (25 mL) and heated at 190 °C for 12 hours. Benzene was evaporated under reduced pressure and compound **13** was purified by silica gel chromatography (eluent: hexane). When necessary, the traces of elemental sulfur were eliminated through precipitation in hexane. This method

allowed for the isolation of compound **13** as a white solid with 13% yield (0.65 g).

M.p. 90–92 °C. ^{1}H-NMR (300 MHz, $CDCl_3$) δ (ppm): 6.96 (s, 2H), 2.36 (s, 6H). ^{13}C-NMR (75 MHz, $CDCl_3$) δ (ppm): 140.1, 130.4, 121.8, 14.7.

Compound 14. Compound **13** (0.4 g, 2.4 mmol) and *N*-iodosuccinimide (0.6 g, 2.6 mmol) were introduced in a three-necked flask under an inert atmosphere. A mixture of chloroform (10 mL) and acetic acid (10 mL) was added and the medium was stirred for 18 hours. Ether (50 mL) was added and the organic phase was washed with a saturated solution of sodium hydrogenocarbonate (3 × 50 mL), a saturated solution of sodium thiosulfate (3 × 50 mL) and brine (3 × 50 mL). The organic phase was dried over magnesium sulfate, filtered and concentrated *in vacuo*. In this manner, compound **14** (524 mg) was isolated with 75% yield.

M.p. 88–90 °C. ^{1}H-NMR (300 MHz, $CDCl_3$) δ (ppm): 7.01–6.98 (m, 1H), 2.33–2.32 (m, 3H), 2.31 (s, 3H). ^{13}C-NMR (75 MHz, $CDCl_3$) δ (ppm): 134.7, 129.9, 124.1, 121.5, 75.1, 16.9, 14.6. MS (ESI^+) *m*/*z*: 294.2 [$M^{+\bullet}$].

Compound 15. Under an argon atmosphere, a solution of malononitrile (375 mg, 5.7 mmol) in dry tetrahydrofuran (2 mL) was added dropwise at 0 °C to a suspension of sodium hydride (60% in mineral oil, 333 mg, 35 mmol) in dry tetrahydrofuran (4 mL). After the addition, the mixture was allowed to warm at room temperature and bis(triphenylphosphine)palladium(II) chloride (199 mg, 0.3 mmol) as well as a solution of 2-iodo-3,6-dimethylthieno[3,2-*b*]thiophene **14** (238 mg, 0.8 mmol) in dry tetrahydrofuran (2 mL). After 60 hours refluxing and cooling to room temperature, chlorhydric acid (1 M, 50 mL) was added. The aqueous layer was extracted with dichloromethane (3 × 50 mL). The combined organic phases were washed with water (2 × 50 mL) and brine (50 mL), dried over magnesium sulfate, filtered and concentrated *in vacuo*. The desired compound was isolated by silica gel chromatography (eluent: dichloromethane) as a brown solid with 27% yield (51 mg). ^{1}H-NMR (300 MHz, $CDCl_3$) δ (ppm): 7.09 (br s, 1H), 5.22 (br s, 1H), 2.46 (d, J = 0.4 Hz, 3H), 2.38–2.36 (m, 3H). MS (MALDI) *m*/*z*: 231.3.

Conflicts of interest

There are no conflicts to declare.

Acknowledgements

The authors are grateful to the University of Angers for its support through an *Arianes* Fellowship as well as the Region Pays de la Loire and Angers Loire Metropole for funding a postdoctoral fellowship through the LUMOMAT program. The authors also acknowledge the PIAM and the SCIAM platforms of the University of Angers for their help. The authors also thank the *Agence Nationale de la Recherche* for granting the FOGEL project and DC is grateful to the *Centre National de la Recherche Scientifique* (CNRS) for a *Délégation* period.

The research led in the Universidad de Zaragoza was financed by MINECO (CTQ2014-52331R) and the Gobierno de Aragón-Fondo Social Europeo (E39). A predoctoral fellowship (FPI BES2009-016966), with EEBB FPI 2012 and 2013, is also acknowledged.

References

1 P. Terech and R. G. Weiss, *Chem. Rev.*, 1997, **97**, 3133.
2 A. R. Hirst, B. Escuder, J. F. Miravet and D. K. Smith, *Angew. Chem., Int. Ed.*, 2008, **47**, 8002.
3 L. E. Buerkle and S. J. Rowan, *Chem. Soc. Rev.*, 2012, **41**, 6089.
4 P. Dastidar, *Chem. Soc. Rev.*, 2008, **37**, 2699.
5 N. M. Sangeetha and U. Maitra, *Chem. Soc. Rev.*, 2005, **34**, 821.
6 A. Vintiloiu and J.-C. Leroux, *J. Controlled Release*, 2008, **125**, 179.
7 D. K. Kumar and J. W. Steed, *Chem. Soc. Rev.*, 2014, **43**, 2080.
8 B. O. Okesola and D. K. Smith, *Chem. Soc. Rev.*, 2016, **45**, 4226.
9 Z. Wei, J. H. Yang, J. Zhou, F. Xu, M. Zrínyi, P. H. Dussault, Y. Osada and Y. M. Chen, *Chem. Soc. Rev.*, 2014, **43**, 8114.
10 X. Yu, L. Chen, M. Zhang and T. Yi, *Chem. Soc. Rev.*, 2014, **43**, 5346.
11 J. Yan, B. S. Wong and L. Kang, in *Soft Fibrillar Materials*, Wiley-VCH Verlag GmbH & Co. KGaA, 2013, p. 129.
12 S. S. Babu, V. K. Praveen and A. Ajayaghosh, *Chem. Rev.*, 2014, **114**, 1973.
13 Z. Zhao, J. W. Y. Lam and B. Z. Tang, *Soft Matter*, 2013, **9**, 4564.
14 *Molecular gels: materials with self-assembled fibrillar networks*, ed. R. G. Weiss and P. Terech, Springer, Dordrecht, 2006.
15 R. J. Kumar, J. M. MacDonald, T. B. Singh, L. J. Waddington and A. B. Holmes, *J. Am. Chem. Soc.*, 2011, **133**, 8564.
16 T. Tu, W. Fang and Z. Sun, *Adv. Mater.*, 2013, **25**, 5304.
17 M. Morimoto, S. Kobatake, M. Irie, H. K. Bisoyi, Q. Li, S. Wang and H. Tian, in *Photochromic Materials, Preparation, Properties and Applications*, ed. H. Tian and J. Zhang, Wiley-VCH, 2016, p. 281.
18 K. Sripathy, R. W. MacQueen, J. R. Peterson, Y. Y. Cheng, M. Dvořák, D. R. McCamey, N. D. Treat, N. Stingelin and T. W. Schmidt, *J. Mater. Chem. C*, 2015, **3**, 616.
19 S. Qu, H. Wang, W. Zhu, J. Luo, Y. Fan, L. Song, H.-X. Zhang and X. Liu, *J. Mater. Chem.*, 2012, **22**, 3875.
20 A. B. Marco, F. Aparicio, L. Faour, K. Iliopoulos, Y. Morille, M. Allain, S. Franco, R. Andreu, B. Sahraoui, D. Gindre, D. Canevet and M. Sallé, *J. Am. Chem. Soc.*, 2016, **138**, 9025.
21 F. Aparicio, L. Faour, D. Gindre, D. Canevet and M. Sallé, *Soft Matter*, 2016, **12**, 8480.

22 G. Zerbi, *Organic Materials for Photonics : Science and Technology*, Elsevier, 1993.
23 A. B. Marco, R. Andreu, S. Franco, J. Garín, J. Orduna, B. Villacampa, B. E. Diosdado, J. T. López Navarrete and J. Casado, *Org. Biomol. Chem.*, 2013, **11**, 6338.
24 X. Tang, L. Pan, K. Jia and X. Tang, *Chem. Phys. Lett.*, 2016, **648**, 114.
25 A. B. Marco, P. Mayorga Burrezo, L. Mosteo, S. Franco, J. Garín, J. Orduna, B. E. Diosdado, B. Villacampa, J. T. López Navarrete, J. Casado and R. Andreu, *RSC Adv.*, 2015, **5**, 231.
26 H.-C. Peng, C.-C. Kang, M.-R. Liang, C.-Y. Chen, A. Demchenko, C.-T. Chen and P.-T. Chou, *ACS Appl. Mater. Interfaces*, 2011, **3**, 1713.
27 K. Takahashi and S. Tarutani, *Heterocycles*, 1996, **43**, 1927.
28 T.-L. Lai, D. Canevet, Y. Almohamed, J.-Y. Mévellec, R. Barillé, N. Avarvari and M. Sallé, *New J. Chem.*, 2014, **38**, 4448.
29 R. Pal, T. Sarkar and S. Khasnobis, *ARKIVOC*, 2012, **1**, 570.
30 G. Melikian, F. P. Rouessac and C. Alexandre, *Synth. Commun.*, 1995, **25**, 3045.
31 K. S. Choi, K. Sawada, H. Dong, M. Hoshino and J. Nakayama, *Heterocycles*, 1994, **38**, 143.
32 J. I. Tietz, J. R. Mastriana, P. Sampson and A. J. Seed, *Liq. Cryst.*, 2012, **39**, 515.
33 P. A. Korevaar, C. Schaefer, T. F. A. de Greef and E. W. Meijer, *J. Am. Chem. Soc.*, 2012, **134**, 13482.
34 For an X-ray crystal structure showing the hindrance resulting from both methyl groups, see: P.-A. Bouit, G. Wetzel, G. Berginc, B. Loiseaux, L. Toupet, P. Feneyrou, Y. Bretonnière, K. Kamada, O. Maury and C. Andraud, *Chem. Mater.*, 2007, **19**, 5325.
35 P. A. Bouit, E. Di Piazza, S. Rigaut, B. Le Guennic, C. Aronica, L. Toupet, C. Andraud and O. Maury, *Org. Lett.*, 2008, **10**, 4159.
36 M. Raynal and L. Bouteiller, *Chem. Commun.*, 2011, **47**, 8271.
37 J. Bonnet, G. Suissa, M. Raynal and L. Bouteiller, *Soft Matter*, 2014, **10**, 3154.
38 Y. Lan, M. G. Corradini, R. G. Weiss, S. R. Raghavan and M. A. Rogers, *Chem. Soc. Rev.*, 2015, **44**, 6035.
39 K. Tiefenbacher, H. Dube, D. Ajami and J. Rebek, *Chem. Commun.*, 2011, **47**, 7341.
40 D. Canevet, A. Pérez Del Pino, D. B. Amabilino and M. Sallé, *J. Mater. Chem.*, 2011, **21**, 1428.
41 Y. Jiang, M. Allain, D. Gindre, S. Dabos-Seignon, P. Blanchard, C. Cabanetos and J. Roncali, *Sci. Rep.*, 2017, **7**, 8317.

